

## High-resolution image-guided tomography and Q-tomography solution for improved depth imaging for an OBC survey

R. Shank Chevron, S. Chattopadhyay, G. Rodriguez, T. Eshete, G. Hilburn, Y. He, and C. VanSchuyver TGS

### Summary

The project area, in the very shallow water of the South Timbalier trench area of the Gulf of Mexico, is known to have complex shallow velocity structure. Seismic waves experience increased attenuation as they travel through the shallow gas-charged mud trench. Amplitude dimming is observed as well as loss of frequency content. We present an improved depth imaging methodology which uses a high-resolution image-guided tomographic solution that addresses the velocity variations and Q tomography and Q migration that address the attenuation problem. The compensation of amplitude and frequency loss helps the model building and improves amplitude fidelity.

### Introduction

The project area, in the very shallow water of the South Timbalier trench area of the Gulf of Mexico, is known to have complex static problems. These issues are addressed as static time shifts from a refraction solution in the time domain. However, a more comprehensive solution is required for depth imaging. We identify two issues present in the data. We observe a sag in the structure and an amplitude dimming as well as a loss of the high frequency contributions below the trench area. But until the velocity is resolved, we cannot identify the source of the dimming as stacking error due to velocity or attenuation. First, we present the application of high-resolution image-guided (IG) tomography to resolve the velocity anomaly and positioning in depth. Once the sag is removed and the data are correctly positioned, we can attribute the dimming to attenuation. Here, we also address these amplitude issues caused by the absorption of seismic waves as they travel through the shallow gas-charged mud trench. Q tomography takes into account the actual dips of the structure and 3D ray paths and is implemented to estimate the attenuation factor. Our main objectives are to address the amplitude and frequency losses below the trench and to produce a more consistent and interpretable image in depth. In this paper we present an enhanced workflow for high-resolution velocity model building and Q compensation on migrated gathers.

### Survey Area

The recently completed 3D OBC covers 933 sq. km, located in the very shallow water in the South Pelto / Grand Isle area of the Gulf of Mexico. (Figure 1) The full azimuth survey was acquired using Sercel SeaRay Ocean-bottom cable with a long inline offset.

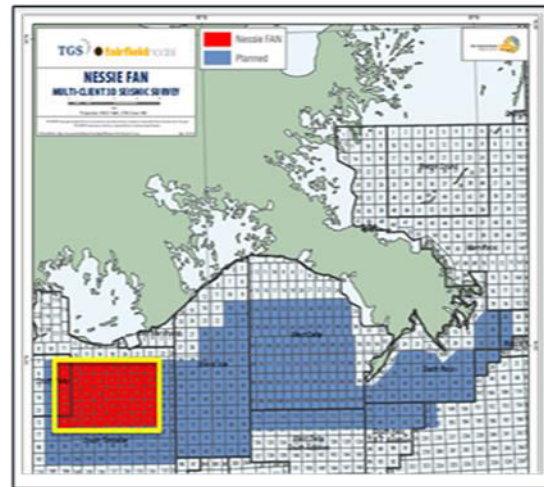


Figure 1 Map of Survey area showing known fields.

### Shallow trench tomography

Prestack depth migration is performed with a calibrated velocity model. A lack of checkshot information in the trench area means that the velocity model does not reflect the low velocity trend present in the trench. This lack of slow velocities results in a migrated image with a significant structural sag (Figure 2).

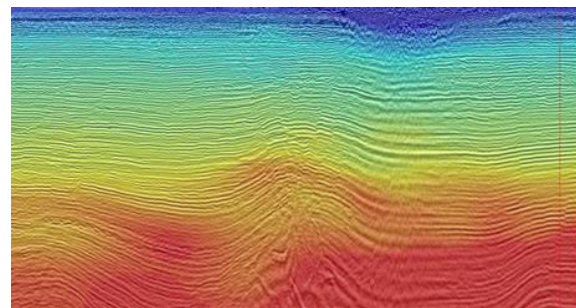


Figure 2 The initial calibrated model.

The 3D OBC data is then azimuthally sectorized, during the binning process, to ensure the full azimuthal illumination of the study area. The input data is sectorized into six azimuths and each is migrated using a TTI prestack Kirchhoff depth migration. To ensure a high-resolution model update at very shallow depths and in the trench area, a finer tomographic inversion grid is adopted. Initially, a single parameter curvature-based residual moveout (RMO) is picked on scanned semblances derived from TTI PSDM

CIGs. We note that a positive curvature (increasing reflection depth with increasing offset) is picked in the trench area, which translates into a velocity decrease. This velocity slowdown is consistent with unconsolidated gas-charged mud. Velocities as low as 1000 m/s result after two tomographic updates (Figure 3). The tomographic updates not only better flatten the CIGs, but dramatically diminish the structural sag (Figure 3). Additionally, faults are better focused, all of which gave more confidence that the velocity updates were converging towards a correct velocity model. (Chattopadhyay et al., 2016)

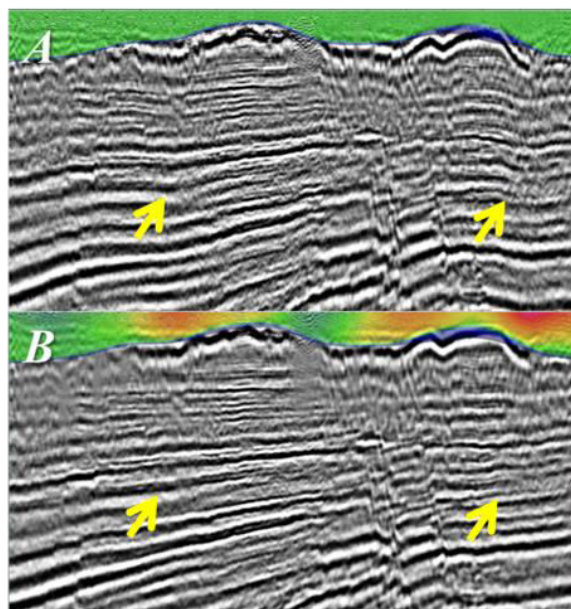


Figure 3 Velocity update in the trench area. (A) Initial model and (B) after shallow high-resolution tomography update.

### High-resolution, image-guided tomography

A higher resolution, geologically conformable model update was achieved by offset-dependent RMO picking and image-guided tomography (IGT). Offset-dependent picking is a robust process utilizing an event-finding technique which is guided by analyzing amplitude variation between traces in the CIGs, geological dips, continuity of the reflector, displacement of events within gathers and a required flatness-constraint. This procedure honors events with complex moveout patterns better than curvature-based picking. More accurately sampling the residual depth error should also allow for better resolution in the velocity model.

The directionality and continuity of events were used to calculate a set of tensors that are used to define update zones whose boundaries are computed by minimizing structure-oriented propagation time within the underlying image. Disruptions in this propagation time identify the coherent and incoherent structures (e.g. faults). The zonal

distribution, computed tensors and the propagation time combine to describe a preconditioning operator for the tomographic inversion. This higher resolution and geologically conformable image-guided tomography (IGT) update produced a higher resolution background sediment velocity model (Figure 4) for depth imaging.

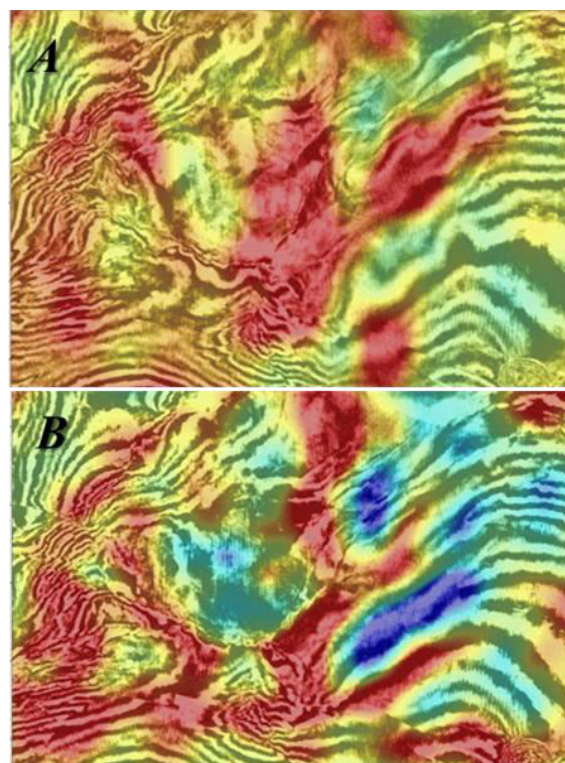


Figure 4 High-resolution, offset-dependent and image-guided tomography velocity at 3500 m depth. (A) with initial model and (B) with updated velocity.

### Amplitude Dimming

Once the structure was resolved, a dimming of the amplitudes and frequencies below the trench is attributed to attenuation. This dimming was identified on both the stack (Figure 5) and the gathers (Figure 6). Figure 5 shows the dimming clearly both visually and in the green spectrum which has both lower amplitude and fewer higher frequencies. In Figure 6, we analyse the amplitude using 3 windows centered on the lines in the image. The graphs above represent the average amplitude of each window on each trace. Here it is obvious that the two gathers in the center, which are beneath the trench, are significantly lower in amplitude.

The extent of the dimming can clearly be seen in the depth slice in Figure 7A. A comparison to a depth slice showing the trench velocity update (Figure 7B) at 300 m reveals that the dimming corresponds well to the trench shape and

### Q tomography

location. The blue line on the depth slice represents the line shown in Figures 5 and 9. The gathers in Figures 6 and 10 are from the locations indicated. The correlation to the gas-charged trench supports the conclusion that the dimming is due to attenuation.

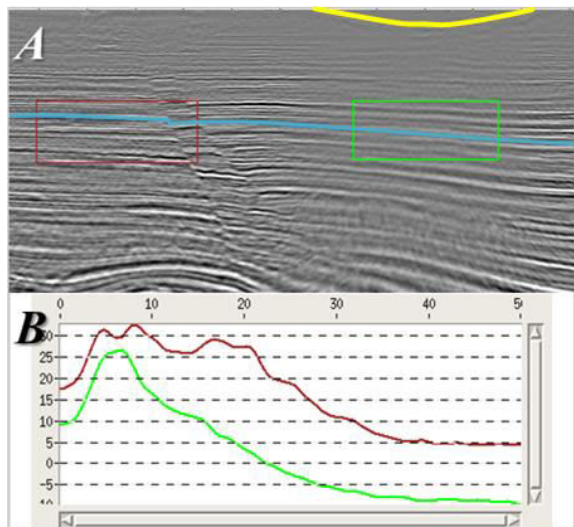


Figure 5 (A) The trench is shown in yellow and the boxes are the location of the frequency analyses (B).

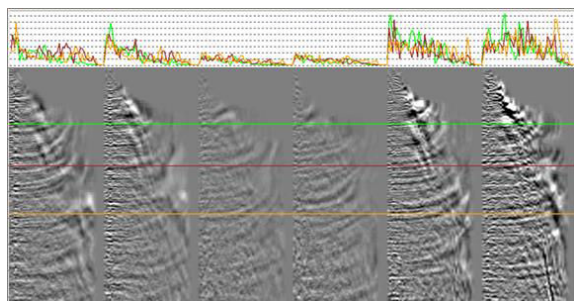


Figure 6 Gathers from the line in Figure 5.

### Q Tomography and Q Migration

Once we confirm that the amplitude and frequency dimming are both related to the trench, we analyze the amplitude at some horizon below the trench to quantify the amplitude and frequency loss. To accurately estimate the Q model, it is necessary to utilize frequency-dependent attenuation information from seismic data. He and Cai (2012) describe a frequency domain tomographic inversion to estimate and correct for frequency-dependent energy attenuation using prestack depth migration gathers. Xin and Hung (2010), describe an amplitude domain inversion to estimate and correct for the amplitude attenuation. We describe an inversion that resolves the amplitude correction as well as the frequency correction. To derive the Q model a smooth interpreted horizon (a regional sand) is used to extract the amplitude variations along the horizon. This horizon is shown, in blue, in Figure 5. The migrated gathers

are used to pick amplitudes for different frequency bands along the horizon. Then the amplitude ratio for three different frequency bands is back-projected along the ray path by implementing 3D tomography.

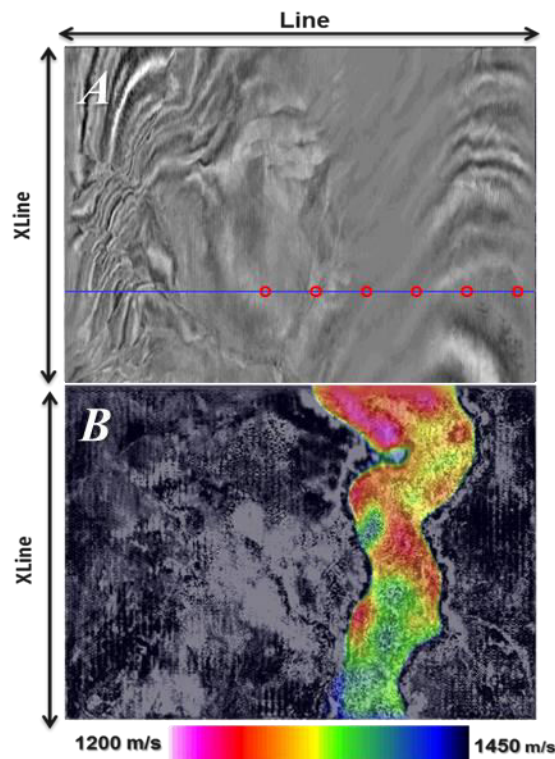


Figure 7 (A) A depth slice showing the amplitude dimming. (B) The trench velocity update.

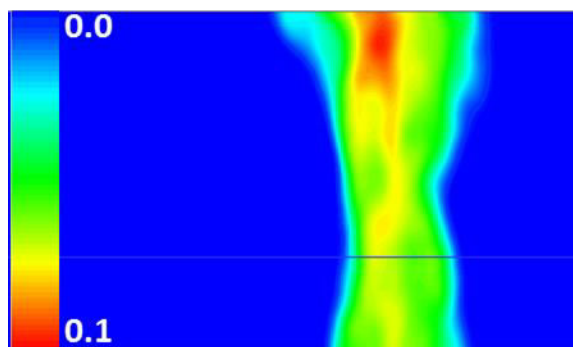


Figure 8 The Q field derived from the Q tomography.

The Q model is obtained by Q tomography, which takes into account the actual dips of the 3D structure and curved ray path in heterogeneous model. In the trench area, depth migrated gathers are used to extract the amplitude variations from three frequency bands and we feed them into a tomographic inversion process to derive a Q field. As expected, the Q field (Figure 8) reflects the shape and location of the reduced amplitude in Figure 7A as well as

## Q tomography

the trench update in Figure 7B. We then incorporate the Q field in a final Q based Kirchhoff depth migration process to compensate for the amplitude loss caused by the inelastic attenuation of seismic waves.

## Examples

A stack after the Q migration (Figure 9A) has no indication of the dimming seen in Figure 5A, and the frequency analyses (Figure 9B) confirm that the amplitude is now recovered in frequency as well. A comparison of the gathers after Q migration (Figure 10) also shows that the amplitude response versus offset is similar for all gathers now rather than having the extreme dimming noted in Figure 6. And finally, the depth slice shown in Figure 11 now gives no indication of the trench in either amplitude or frequency.

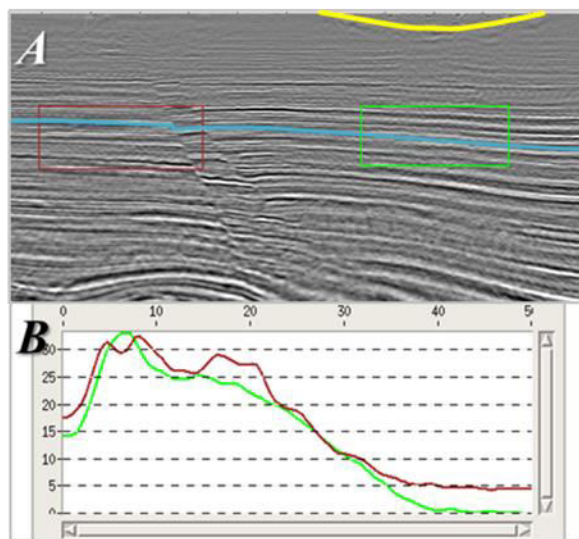


Figure 9 (A) Stack after Q migration. (B) Frequency analyses of the stack.

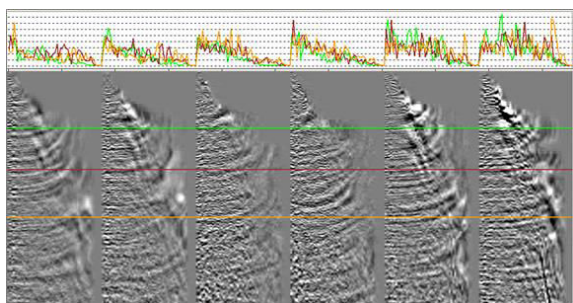


Figure 10 Gathers after Q migration, same NMO as Figure 6.

## Conclusions

The velocity model building was addressed by offset-dependent picking and IG tomography which resulted in

higher resolution and a geologically conformable model update with a) better focused and improved sub-trench events b) improved fault imaging in the whole project area. Also, we demonstrate the significant improvements made through the derivation of a Q Field and its application to correct both amplitude and frequency with Q migration. In addition to the amplitude and frequency improvements in the stack, the gathers demonstrate an improved AVO response as well. Overburden transmission loss is common in the Deepwater assets and these types of corrections could help in the understanding and characterization of the reservoirs and help define future opportunities.

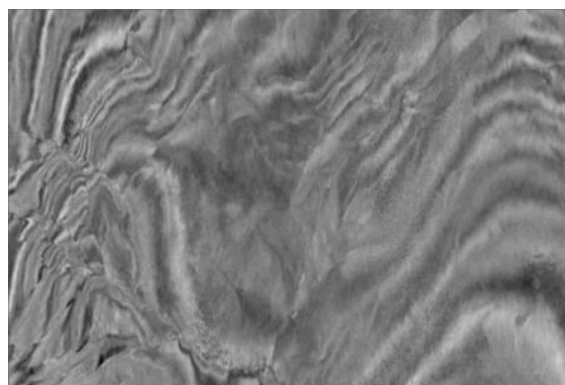


Figure 11 Depth slice after Q migration.

## Acknowledgements

The authors are grateful to Chevron and TGS for permission to include the Nessie data in this abstract. We wish to thank George Rhodes, Jr., Randy Storey, Joshua Richardson and Katy Lohr of Chevron; and Ashley Lundy, Steve Hightower, Sampad Laha, Kenny Lambert, George Cloudy, Jr., Bin Wang and Zhiming Li of TGS for their support and suggestions. The Nessie survey is a cooperative effort between TGS and Fairfield. The Q correction processing was performed for Chevron.

#### **EDITED REFERENCES**

Note: This reference list is a copyedited version of the reference list submitted by the author. Reference lists for the 2017 SEG Technical Program Expanded Abstracts have been copyedited so that references provided with the online metadata for each paper will achieve a high degree of linking to cited sources that appear on the Web.

#### **REFERENCES**

- Chattopadhyay, S., 2016, High-resolution image-guided tomographic solution for improved imaging in ultrashallow water trench area of Gulf of Mexico: 86th Annual International Meeting, SEG, Expanded Abstracts, 5234–5238, <http://dx.doi.org/10.1190/segam2016-13950552.1>.
- He, Y., and J. Cai, 2012, Q tomography towards true amplitude image and improve sub-karst image: 82nd Annual International Meeting, SEG, Expanded Abstracts, 1–5, <http://dx.doi.org/10.1190/segam2012-1220.1>.
- Xin, K. and B. Hung, 2010, 3-D tomographic Q inversion for compensating attenuation anomalies: 21st Geophysical Conference, ASEG, Extended Abstracts, 1–4, <https://doi.org/10.1071/ASEG2010ab075>.